

Functional Properties of Sensory Nerve Terminals of the Mouse Cornea

Omar González-González,¹ Federico Bech,¹ Juana Gallar,² Jesús Merayo-Llaves,¹ and Carlos Belmonte^{1,2}

¹Instituto Universitario Fernández-Vega, Universidad de Oviedo & Fundación de Investigación Oftalmológica, Oviedo, Spain

²Instituto de Neurociencias, Universidad Miguel Hernández-Consejo Superior de Investigaciones Científicas, San Juan de Alicante, Spain

Correspondence: Carlos Belmonte, Instituto Universitario Fernández-Vega, Avda. Dres. Fernández-Vega, 34, 33012 Oviedo, Spain; carlos.belmonte@umh.es.

Submitted: May 31, 2016

Accepted: November 13, 2016

Citation: González-González O, Bech F, Gallar J, Merayo-Llaves J, Belmonte C. Functional properties of sensory nerve terminals of the mouse cornea. *Invest Ophthalmol Vis Sci*. 2017;58:404–415. DOI:10.1167/iivs.16-20033

PURPOSE. To define the firing properties of sensory nerve terminals innervating the adult mouse cornea in response to external stimuli of differing modality.

METHODS. Extracellular electrical activity of single corneal sensory nerve terminals was recorded in excised eyes of C57BL/6J mice. Eyes were placed in a recording chamber and were continuously superfused with warm saline solution. Nerve terminal impulse (NTI) activity was recorded by means of a glass pipette (tip ~ 50 μm), applied on the corneal surface. Nerve terminal impulse discharges were stored in a computer for offline analysis.

RESULTS. Three functionally distinct populations of nerve terminals were identified in the mouse cornea. Pure mechanonociceptor terminals (9.5%) responded phasically and only to mechanical stimuli. Polymodal nociceptor terminals (41.1%) were tonically activated by heat and hyperosmolar solutions (850 mOsm·kg⁻¹), mechanical force, and/or TRPV1 and TRPA1 agonists (capsaicin and allyl isothiocyanate [AITC], respectively). Cold-sensitive terminals (49.4%) responded to cooling. Approximately two-thirds of them fired continuously at 34°C and responded vigorously to small temperature reductions, being classified as high-background activity, low-threshold (HB-LT) cold thermoreceptor terminals. The remaining one-third exhibited very low ongoing activity at 34°C and responded weakly to intense cooling, being named low-background activity, high-threshold (LB-HT) cold thermoreceptor terminals.

CONCLUSIONS. The mouse cornea is innervated by trigeminal ganglion (TG) neurons that respond to the same stimulus modalities as corneal receptors of other mammalian species. Mechano- and polymodal endings underlie detection of mechanical and chemical noxious stimuli while HB-LT and LB-HT cold thermoreceptors appear to be responsible for basal and irritation-evoked tearing and blinking, respectively.

Keywords: corneal sensory nerves, thermoreceptors, corneal innervation, polymodal nociceptors, mechanonociceptors

The use of mice in biomedical studies is receiving growing attention due to the ample possibilities of genetic manipulation offered by this species. Such interest extends also to the eye, and in recent years, many publications have used mice to analyze normal and pathologic ocular processes, including those affecting the sensory innervation of the corneal surface.¹⁻³

As a result of these studies, the distribution and architecture of mouse corneal sensory innervation is reasonably well known, confirming that it follows the morphologic pattern of corneal nerve branching described in other mammalian species,^{4,5} although remarkable differences exist in nerve density between mice strains.⁴ Additionally, the corneal innervation of mice has been used to explore the origin and trophic dependence of peripheral sensory nerves during prenatal development⁶ and postinjury nerve regeneration in adults,^{3,7,8} as well as age-dependent changes in the architecture and function of corneal nerves.^{2,9} Moreover, mice have been extensively employed to define the morphologic alterations of corneal nerves caused by a number of pathologic conditions such as diabetes,¹⁰ surgical injury,^{1,11,12} herpes virus infections,^{13,14} and dry eye disease.^{15,16}

In contrast to the ample knowledge of the anatomy of the corneal innervation in mice, its functional characteristics are still poorly defined. Impulse activity of mouse corneal sensory axons and nerve terminals has been recorded in a few studies, and these were mainly centered on the population of low-threshold cold thermoreceptors, whose electrical activity is easiest to record and characterize.^{9,17-19}

Electrophysiological experiments in other species (cat, rabbit, guinea pig, rat) firmly established that the cornea is functionally innervated by the peripheral axons of three distinct classes of peripheral sensory receptor neurons: mechanosensory, responding only to mechanical forces; polymodal nociceptor, activated by mechanical stimuli as well as heat and a variety of endogenous and exogenous chemicals; and cold thermoreceptor neurons, primarily excited by moderate cooling and hyperosmolar solutions.²⁰⁻³⁶ In the present work, we performed a systematic analysis of the firing properties of the various functional classes of sensory nerve terminals innervating the adult mouse cornea and defined their functional properties and firing pattern in response to stimuli of differing modality.



METHODS

All experiments were conducted in accordance with the ethical guidelines of the ARVO Statement for the Use of Animals in Ophthalmic and Vision Research and the European and Spanish regulations on the protection of animals used for research, and followed a protocol approved by the Ethics Committee of the University of Oviedo. Animals were euthanized with an overdose of sodium pentobarbital (Dolethal; Vetoquinol, Lure, France) injected intraperitoneally.

Recordings of single corneal nerve terminals *in vitro* were performed as described in previous studies.^{17,35} The posterior pole of the eyeball and optic nerve was introduced into a silicone tube located at the bottom of a recording chamber filled with saline and secured in place by continuous suction. The eye was continuously superfused with a physiological saline solution of the following composition (in mM): NaCl (128), KCl (5), NaH₂PO₄ (1), NaHCO₃ (26), CaCl₂ (2.4), MgCl₂ (1.3), and glucose (10). The solution was bubbled with a gas mixture (5% CO₂ and 95% O₂) and maintained at the desired temperature (~34°C) with a home-made Peltier device. A borosilicate glass micropipette electrode with a tip diameter of approximately 50 μm filled with saline solution was gently placed in contact with the corneal surface, using a micromanipulator. Light suction was then applied through the pipette to produce a high-resistance seal with the corneal surface, to allow recording of nerve impulses generated at single nerve terminals located beneath the electrode tip. An Ag-AgCl electrode in the recording chamber served as the indifferent electrode. Nerve terminal impulses (NTIs) were amplified with an AC amplifier (Neurolog NL104; Digitimer, Welwyn, UK) and stored at 10 kHz in a computer, using a CED micro 1401 interface and Spike 2 software (both from Cambridge Electronic Design, Cambridge, UK). Only recordings containing NTIs originating from a single nerve terminal were analyzed. At these sites the NTIs were clearly distinguished from noise (~10 μV peak to peak) and had similar amplitudes and waveforms indicating that they originated from the same sensory nerve ending. To minimize deterioration of the preparation with time, the total duration of the experiment was limited to a maximum of 5 hours.

Solutions

Menthol (Sigma-Aldrich Corp., St. Louis, MO, USA) was prepared as a 20 mM stock solution in ethanol and diluted to a final concentration of 20 μM with saline solution. Capsaicin (Sigma-Aldrich Corp.) was prepared as a 1 mM stock solution in ethanol and diluted to a final concentration of 1 μM with saline solution. Allyl isothiocyanate (Sigma-Aldrich Corp.) was prepared as a 100 mM stock solution in dimethyl sulfoxide (DMSO) and diluted with the saline solution to a final concentration of 100 μM. Hyperosmolar solutions were prepared by adding NaCl (3 M) to the physiological saline solution (310 ± 1.5 mOsm·kg⁻¹) until reaching the desired osmolality values (340, 400, and 850 mOsm·kg⁻¹), measured with a freezing point osmometer (OSMOSTAT OM-6020; Kyoto Daiichi, Kyoto, Japan). The “inflammatory soup”¹⁸ contained the following substances dissolved in saline solution: bradykinin (5 μM), histamine (100 μM), PGE₂ (10 μM), 5-HT (100 μM), and ATP (100 μM), all from Sigma-Aldrich Corp.

Experimental Protocol

In order to obtain an estimation of the relative density of the different functional types of corneal terminals, the recording pipette was placed at sequential points on the corneal surface separated by an approximate distance of 0.2 mm, and aligned

at the intersections of a 6 by 3 grid formed by evenly spaced straight lines going between opposite sides of the limbal border (Figs. 1A, 1B). First, one half of the cornea was explored for nerve activity, and the eye was then rotated and the opposite half of the cornea was explored. After application of the pipette to the corneal surface, responses to cold or mechanical stimuli were assessed. The appearance of spontaneous or stimulus-evoked NTI activity at the recording site was used to ascertain success in detecting an active sensory nerve terminal. If no spontaneous or cold- or mechanically evoked activity was obtained, the electrode was moved to the next recording point. Responsiveness to mechanical stimulation was assessed with a gentle forward displacement (10 μm) of the recording electrode with the micromanipulator. Thereafter, thermal and chemical stimuli were sequentially applied. The same general protocol was applied to sensory terminals of all modalities.

Cold stimulation was first performed by decreasing the background temperature of the perfusion solution from 34°C down to ~14°C. This generated a cooling ramp lasting ~35 seconds at mean cooling rate of ~0.6°C·s⁻¹. When the peak temperature fall was attained, warming was applied to return to the basal temperature at a similar speed. After a resting period of 120 seconds, a mechanical stimulation was made, applying pressure with the pipette with a 10-μm forward displacement of the tip of the electrode for 2 or 15 seconds. The number of NTIs evoked during the stimulation period was counted.

After another 120 seconds, a heating ramp from 34°C to ~52°C at 0.5°C·s⁻¹ (~30-second duration) was applied, and when the peak value was reached, temperature was returned to 34°C at a similar rate.

Chemical stimulation was initiated after a resting period of at least 300 seconds, by switching the perfusion with control saline solution at 34°C to a saline solution containing the drug at 34°C. Menthol (20 μM) was always tested first. Two minutes after the onset of the perfusion with menthol, a cooling ramp down to ~14°C was applied to explore the presence of menthol-induced sensitization of the cold response. After warming back to 34°C, the cornea was washed with the control saline solution for a period of at least 5 minutes. Afterward, stimulation with one or several other test solutions (AITC, “inflammatory soup,” hyperosmolar solutions) was sequentially performed using the same protocol: Namely, after a control recording period of 2 minutes, perfusion with the test solution for 2 to 3 minutes was initiated, including a cooling ramp, followed by a washing time of at least 5 minutes. Capsaicin (1 μM) was applied whenever possible for 2 to 3 minutes at 34°C, always at the end of experiment due to the strong inactivating effect of this drug.

Analysis of NTI Activity

The following parameters of the NTI activity were analyzed. Background activity, defined as the mean basal ongoing frequency in impulses per second (imp·s⁻¹) at the basal temperature (33.9 ± 0.07°C), was measured during the 30-second period that preceded the onset of a stimulus. Cooling threshold was the temperature (°C) value during a cooling ramp at which NTI frequency in imp·s⁻¹ increased to a value greater than the value of the mean basal NTI frequency during the 10-second period preceding the onset of a cooling ramp, plus three times its standard deviation. Cooling response was mean NTI frequency during cooling. Maximum response to cold was the highest-frequency value measured during a cooling ramp (imp·s⁻¹). Silencing temperature was temperature (°C) needed to silence NTI firing during a cooling ramp. Response to heat was the total number of NTIs during 30

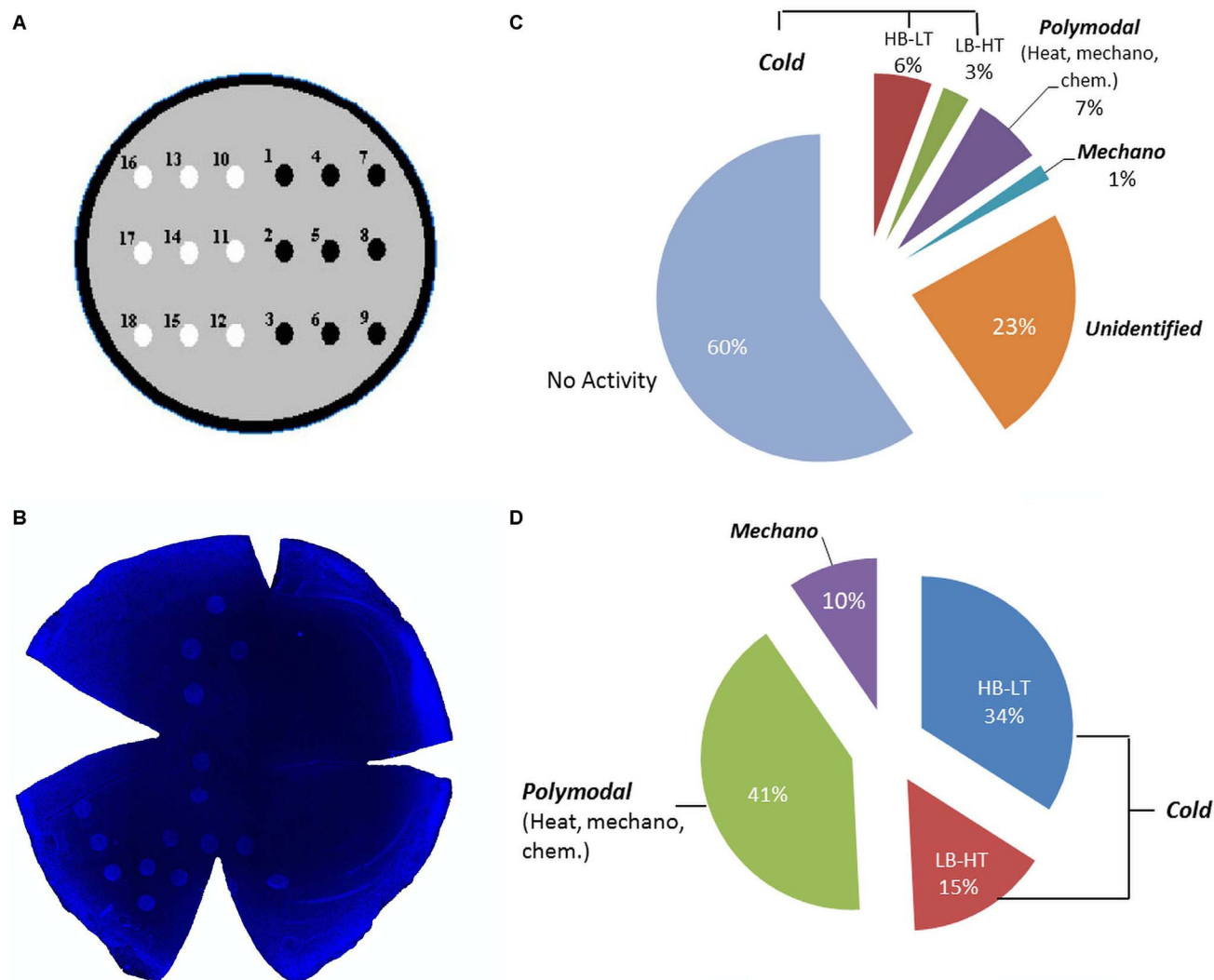


FIGURE 1. (A) Schematic representation of the cornea to show the location and sequence of points at which the recording electrode was placed during the experiment. (B) Picture of an excised cornea, showing the marks left by the recording electrode tip on the epithelial surface. (C) Probability of finding NTI activity associated with the different modalities of stimuli. (D) Percent of terminals belonging to the different functional classes of corneal receptor terminals identified in all experiments.

seconds following the onset of the heating ramp. Comparison was made with the number of NTIs during the 30-second period immediately preceding the heating ramp. Heating threshold was temperature ($^{\circ}\text{C}$) value during a heating ramp at which NTI frequency in $\text{imp}\cdot\text{s}^{-1}$ increased to a value greater than the value of the mean basal NTI frequency during the 30-second period preceding the onset of a heating ramp, plus three times its standard deviation. Mechanical response was the total number of NTIs during 10 seconds following the onset of mechanical stimulation. As a control, the total number of NTIs fired during the 10-second period immediately prior to mechanical stimulation was used. Chemical response, the mean firing frequency (in $\text{imp}\cdot\text{s}^{-1}$) during the last 30 seconds of perfusion with the test substance (AITC, capsaicin, inflammatory soup, menthol, hyperosmolal solutions), was measured and compared with the NTI firing frequency during the 30-second period preceding chemical stimulation.

Statistical Analysis

Data from NTI recordings were exported from Spike 2 (CED) to Origin 8 software for analysis. Statistical comparisons were

performed using Microsoft Excel 2010 (Microsoft Corporation, Redmond, WA, USA), Origin 8 (OriginLab Corporation, Northampton, MA, USA), and InStat 3 (GraphPad Software, Inc., La Jolla, CA, USA). Paired Student's *t*-test was used unless the characteristics of the data distribution required the use of the nonparametric Wilcoxon signed-rank test, as indicated in the text. Values are expressed as mean \pm standard error (SE) of the mean, with *n* denoting the number of terminals.

RESULTS

Experiments were performed in 124 eyes obtained from 62 young adult mice of both sexes (3–6 months of age). A mean of 15 points per cornea were explored.

Based on the response characteristics to different stimuli, corneal sensory terminals were classified as high-threshold mechanoreceptor, polymodal nociceptor, and cold thermoreceptor terminals. Figures 1C and 1D show the proportion of successful attempts, that is, those in which NTIs were detected, as well as the percentage of each functional class of terminal. In more than half of the recording points, no NTI

TABLE 1. Functional Characteristics of Mechanonociceptor and Polymodal Nociceptor Terminals

NTI Activity Parameter	Terminal Type	
	Mechanonociceptor	Polymodal Nociceptor
Success, %	1.6	6.9
Cooling response, No. NTI/30 s		
Before	7.7 ± 4.7 <i>n</i> = 3	8.4 ± 1.4 <i>n</i> = 50
During	7.7 ± 6.7 <i>n</i> = 3	3.9 ± 0.7 <i>n</i> = 50
Mechanical stimulation, No. NTI/10 s		
Before	2.5 ± 1.7 <i>n</i> = 4	1.9 ± 0.5 <i>n</i> = 38
During	22.3 ± 4.5 <i>n</i> = 4	14.3 ± 1.4 <i>n</i> = 38
Heating response, No. NTI/30 s		
Before	10 ± 8.5 <i>n</i> = 3	6 ± 0.9 <i>n</i> = 48
During	5 ± 2.1 <i>n</i> = 3	30.2 ± 2.4 <i>n</i> = 48
Chemical stimulation, Δ imp·s ⁻¹		
100 μM AITC	nd	0.3 ± 0.1 <i>n</i> = 4
1 μM capsaicin	nd	1.6 ± 0.2 <i>n</i> = 23
Hyperosmolal 850 mOsm	nd	0.38 ± 0.09 <i>n</i> = 5

Success % indicates the percentage of successful attempts of recording a terminal from each group with regard to the total number of attempts. The cooling, heating, and mechanical response are expressed as the total number of NTIs during the 30 seconds immediately before and the 30 seconds during the cooling and the heating ramp, and 10 seconds immediately before and during the first 10 seconds of the mechanical pulse, respectively. Chemical stimulation is expressed as the difference increment of activity in the 30 seconds of maximum activity during the 2 to 3 minutes of chemical perfusion with regard to the 30 seconds immediately before (see Methods). nd, no response or quantitative data available.

activity was observed; in an additional 23% of trials, the impulses had small amplitude, preventing reliable identification and quantitative analysis of the nerve terminal characteristics.

Mechanoreceptor Terminals

Some terminals (9.5%) responding exclusively to mechanical stimulation were found (Table 1). Two of them had very low frequency of ongoing activity (0.1 and 0.5 imp·s⁻¹, one of them increased its basal activity after the different experimental maneuvers) while the rest remained silent during the 30-second background activity measuring period prior to stimulation. Pushing the recording pipette against the corneal surface for 2 seconds evoked a burst of NTIs that stopped immediately with the removal of the pipette's pressure (Figs. 2A, 2C). A similar, transient NTI firing response was obtained when pressure was maintained for 15 seconds (Fig. 2C). The mean number of NTIs fired during this stimulus was 22.3 ± 4.5 (*n* = 4).

Polymodal Nociceptor Terminals

Of the nerve terminals exhibiting a very low or no activity during the initial recording period, 41.1% responded to heat and generally also to mechanical pressure as well as to one or

more of the chemical stimuli (Table 1). In the absence of an applied stimulus, the mean spontaneous activity of these polymodal nociceptor terminals was 0.3 ± 0.04 (*n* = 50; range, 0.02–1.5 imp·s⁻¹).

Thermal Stimulation. Application of a 30-second cooling ramp (from 34°C to 13.7 ± 0.3°C) to polymodal terminals reduced their ongoing activity, so that the mean number of NTIs fired during the cooling ramp was significantly lower than during the 30-second period before applying the cold stimulus (8.4 ± 1.4 NTIs before versus 3.9 ± 0.7 NTIs during the cooling ramp, *n* = 50, *P* < 0.001; Table 1; Fig. 3).

In contrast, in response to a 30-second heating ramp (from 33.7 ± 0.1°C to 52.0 ± 0.2°C, *n* = 48), polymodal terminals showed a marked increase in their firing frequency (Table 1), sometimes adopting a bursting pattern (Fig. 3). The heating threshold was 41.5 ± 0.5°C (*n* = 48). However, such threshold temperature value for the heating response varied widely among individual terminals, ranging between 36.3°C and 51.4°C. Also, the frequency and duration of the NTI discharge differed between the nerve terminals, although, in all cases, NTI activity silenced completely at the onset of cooling at the termination of the heating ramp. The magnitude of the response to heating, measured as the total number of impulses fired during the complete duration of the heating ramp, was 30.2 ± 2.4 NTIs, a value significantly higher than during the 30-second period at 34°C that preceded the heat ramp (6.0 ± 0.9 NTI *n* = 48, *P* < 0.001, Table 1). Around 14% of the polymodal terminals became silent and irresponsive after the first heating stimulus, whereas the rest resumed activity approximately 2 minutes after the end of the heat-evoked NTI discharge, with their activity before and after heating being similar (0.2 ± 0.02 imp·s⁻¹ and 0.15 ± 0.03 imp·s⁻¹, respectively, *n* = 43, *P* > 0.05). In 11 of 18 tested terminals, a second heat ramp was applied 5 to 10 minutes later. In four of them no firing response was evoked; that is, they had been inactivated by the first heating ramp. In the remaining seven terminals, sensitization developed. This appeared either as a drop in heating threshold to -3.3 ± 0.4°C below the value determined during the first heat ramp (*n* = 3), as an increase in the total number of impulses during the heating pulse without change in threshold (*n* = 3), or as a threshold reduction combined with an increase in firing (*n* = 1).

Mechanical Stimulation. Mechanical stimulation for 2 seconds activated 38 of 44 polymodal terminals, classified as such by their activation by heat and/or chemical stimuli. The mechanically activated polymodal receptor terminals generated a short burst of NTIs at the onset of the maneuver (Fig. 3). On average, 14.3 ± 1.4 NTIs (*n* = 38) were counted during the 10-second period following the onset of the stimulus, a value that was significantly higher than that counted during the 10 seconds prior to the application of the stimulus (1.9 ± 0.5 NTIs, *n* = 38, *P* < 0.001, Wilcoxon matched-pairs test). In seven of the polymodal terminals responding to mechanical stimulation, the stimulus was repeated 2 minutes later but on this occasion was maintained for 15 seconds. The firing response was again transient, being composed of an initial burst of NTIs lasting for 1 to 2 seconds that returned to the basal firing level for the remainder of the stimulus; the total number NTIs during the first 10 seconds of the mechanical stimulus (9.3 ± 2.1, *n* = 7) was not significantly different from that measured in response to the 2-second stimulus (see above).

Chemical Stimulation. To define chemosensitivity of polymodal terminals, various chemical agents were applied to terminals that previously responded to a heat ramp (Fig. 3). Table 1 summarizes the response of polymodal terminals to the different chemical stimuli tested. Hyperosmolal solutions were tried in a total of 23 terminals (Table 1). The ongoing activity

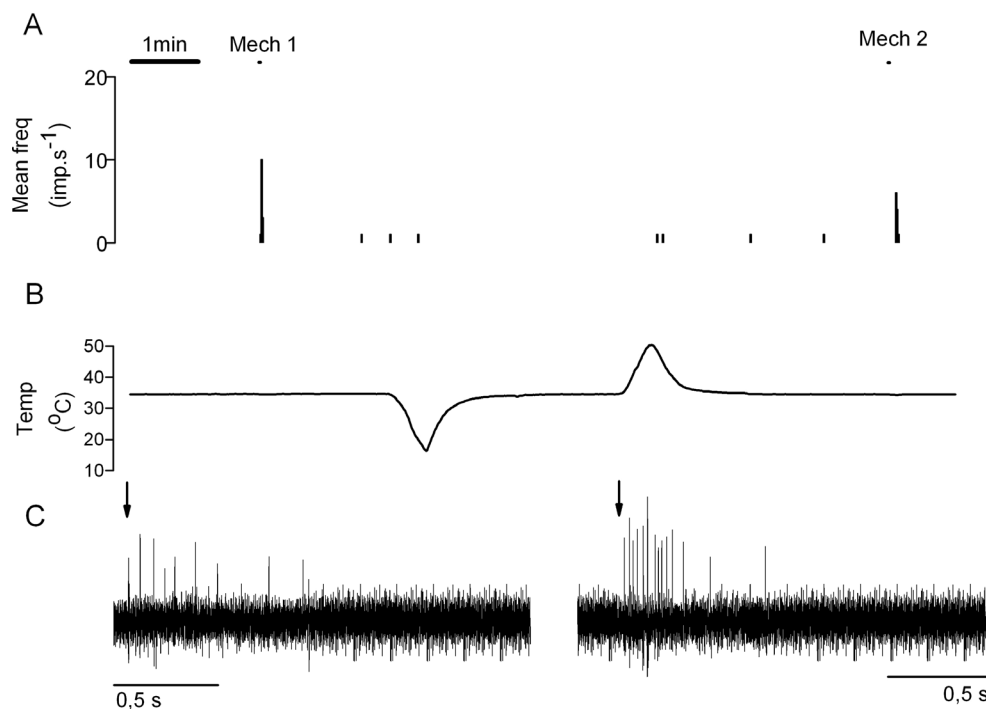


FIGURE 2. Example of NTI activity in a mechanonociceptor terminal. **(A)** Time histogram of the NTI discharge evoked by a 2-second (Mech 1) or a 15-second (Mech 2) forward displacement ($10\ \mu\text{m}$) of the recording electrode. **(B)** Temperature record of the perfusing solution during the same time period shown in **(A)**. **(C)** Samples of the recordings of NTI impulse activity evoked in the same mechanonociceptor terminal by a displacement of the electrode during a 2-second (*left*) and a 15-second (*right*) mechanical stimulation. *Arrows* indicate the onset of the stimulus.

increased during perfusion with $850\ \text{mOsm}\cdot\text{kg}^{-1}$ solution from 0.2 ± 0.1 to a mean value of $0.5 \pm 0.1\ \text{imp}\cdot\text{s}^{-1}$ ($n = 5$, $P < 0.05$). Also, when this high-osmolality solution was applied, the NTI irregular firing pattern changed to a bursting pattern and

the shape of NTIs was altered, becoming wider and of smaller amplitude (data not shown; see also Ref. 35). The TRPA1 agonist AITC ($100\ \mu\text{M}$) was tested in 9 terminals and weakly activated 4 of them, while the TRPV1 agonist capsaicin ($1\ \mu\text{M}$)

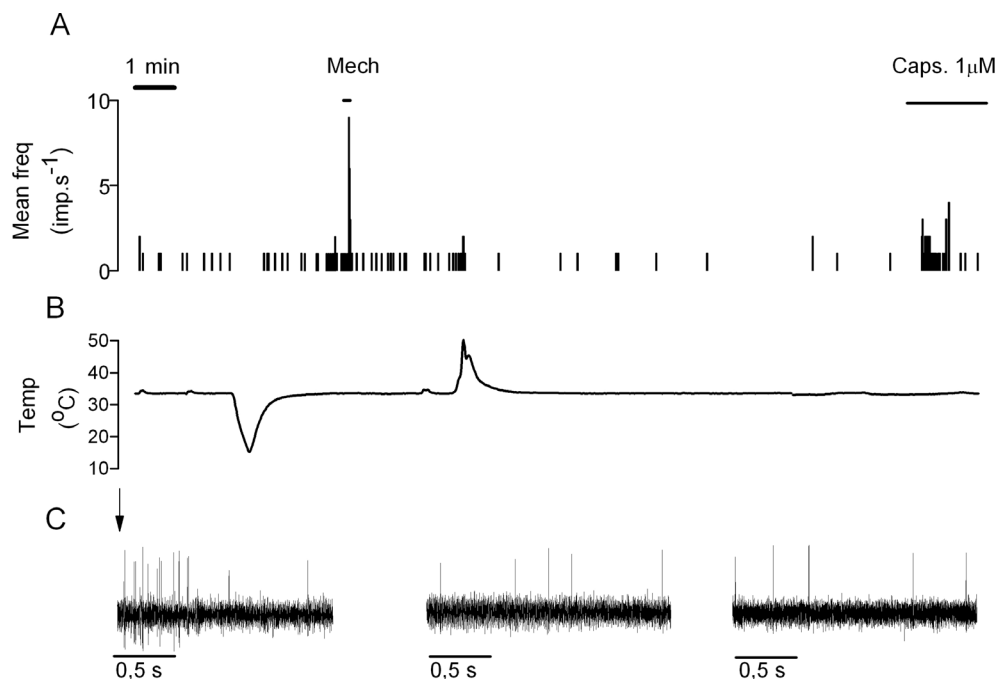


FIGURE 3. Example of the NTI response of a polymodal nociceptor terminal. **(A)** Time histogram of the NTI discharge of a polymodal nociceptor terminal evoked by a $10\text{-}\mu\text{m}$ forward displacement of the recording electrode for 2 seconds (Mech), changes in bath temperature (see record of temperature of perfusion solution in **[B]**), and perfusion with $1\text{-}\mu\text{M}$ capsaicin. **(C)** Sample records of the NTI impulse activity during a 2-second mechanical stimulation (*left trace*), at the beginning of the response in heating ramp (*center trace*), and during the perfusion with capsaicin (*right trace*), in the same polymodal nociceptor. *Arrow* indicates the onset of the mechanical stimulus.

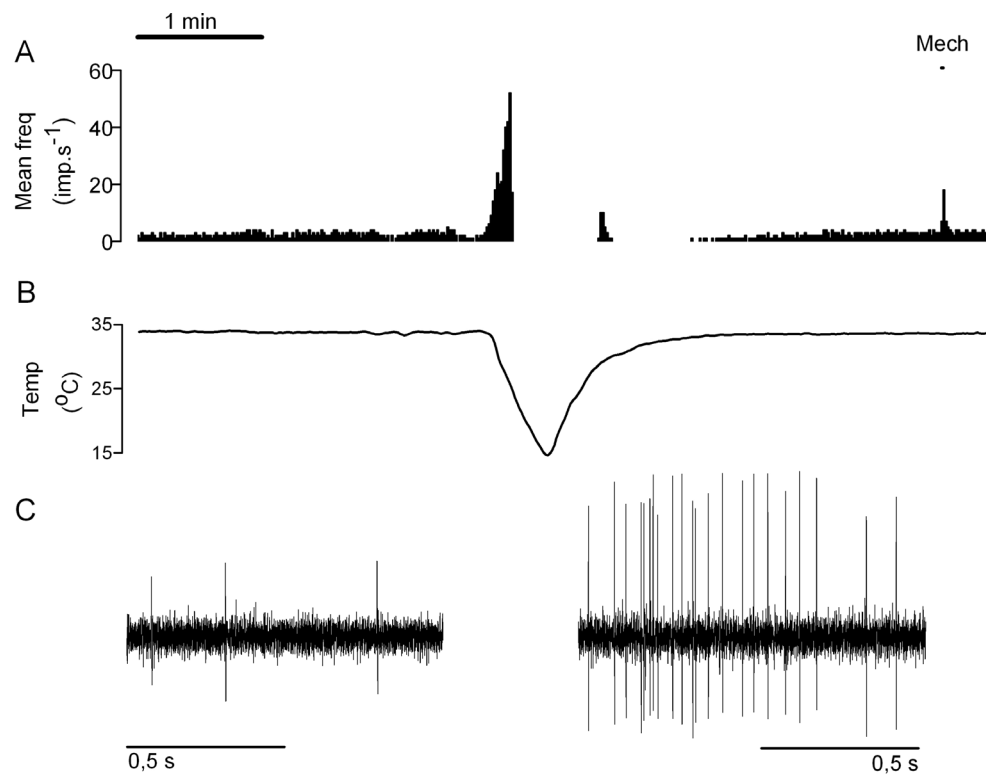


FIGURE 4. Example of the NTI response of a HB-LT cold thermoreceptor terminal to a cooling ramp. (A) Time histogram of the NTI discharge. Notice the transient firing observed during temperature recovery (see text). Mech, mechanical stimulation (10- μ m forward displacement of the electrode for 2 seconds). (B) Bath temperature trace during the same time period shown in (A). (C) Sample records of the NTI impulse activity during control recording at 34°C (*left*) and during the mechanical stimulation (*right*) in the same HB-LT terminal.

activated 23 of the 24 terminals tested ($0.1 \pm 0.04 \text{ imp}\cdot\text{s}^{-1}$ before and $1.4 \pm 0.2 \text{ imp}\cdot\text{s}^{-1}$ during capsaicin application, $P < 0.001$). Application of inflammatory soup (see Methods) to seven polymodal terminals for 5 minutes evoked a significant increase in the ongoing NTI firing rate (from 0.1 ± 0.02 to $0.2 \pm 0.04 \text{ imp}\cdot\text{s}^{-1}$, $P < 0.003$).

Cold Thermoreceptor Terminals

Corneal terminals responding to cooling represented a 49.4% of the total.

High-Background/Low-Threshold (HB-LT) Cold-Sensitive Terminals. All nerve terminals exhibiting a repetitive background activity immediately after application of the pipette also responded readily to a cooling ramp with a robust increase in firing frequency. We classified these nerve terminals as high-background activity, low-threshold (HB-LT) cold thermoreceptor terminals; they represented 72% of the total population of cold-sensitive nerve endings found in the cornea. Mechanical pressure evoked a few NTIs in six HB-LT terminals where it was tested (Fig. 4). Table 2 summarizes the firing characteristics of the HB-LT cold thermoreceptor terminals. Their background activity at 34°C was usually composed of regularly appearing individual or paired NTIs, firing at a mean frequency ranging between 1.3 and 19.3 $\text{imp}\cdot\text{s}^{-1}$ (mean $6.6 \pm 1.0 \text{ imp}\cdot\text{s}^{-1}$, $n = 26$). During the initial portion of the cooling ramp, firing pattern often changed from regular beating to bursting and, after reaching a peak frequency value of $57.8 \pm 3.9 \text{ imp}\cdot\text{s}^{-1}$ at $26 \pm 0.7^\circ\text{C}$, NTIs usually silenced at around 23°C, well before reaching the lowest temperature point (14–15°C). During the 30-second heating period back to the control temperature, a transient NTI discharge (mean number 102.1 ± 40 NTIs), appearing at a mean temperature of $27.5 \pm 0.5^\circ\text{C}$

and lasting on the average 7.5 ± 1.8 seconds, was observed in 14 out of 26 HB-LT terminals (Fig. 4), followed again by a silence until a temperature of $31.4 \pm 0.3^\circ\text{C}$ was attained, at which point the NTI activity gradually recovered to the frequency that it had prior to the cooling ramp. The application of 20 μM menthol increased significantly ongoing activity of HB-LT terminals (Table 2). Also, perfusion with 340 $\text{mOsm}\cdot\text{kg}^{-1}$ hyperosmolar solution increased the ongoing firing frequency (from 8.0 ± 1.5 to $10.3 \pm 1.6 \text{ imp}\cdot\text{s}^{-1}$, $P < 0.05$). Sixty-seven percent of the HB-LT terminals responded to a heating ramp with a transient NTI discharge (“paradoxical response”) starting at $41.9 \pm 2^\circ\text{C}$ (mean number of NTIs, 355.5 ± 111.4 ; mean duration of the firing period, 9.4 ± 2.1 seconds). Four HB-LT terminals with a paradoxical response were tested with 1 μM capsaicin; in all of them, capsaicin increased the mean firing rate at 34°C ($\Delta = 13.0 \pm 3.5 \text{ imp}\cdot\text{s}^{-1}$, $n = 4$) and reduced the cooling threshold to temperature values 3°C to 4°C lower than the pretreatment value. Intriguingly, in two out of four terminals tested, the TRPA1 agonist AITC prolonged the duration of NTI firing during the cooling ramp to a temperature below 20°C (19.9°C and 14.4°C in the two responsive terminals).

Low-Background/High-Threshold (LB-HT) Cold-Sensitive Terminals. Among corneal terminals exhibiting a very low initial background activity at 34°C, a proportion were characterized by the firing of a sustained NTI discharge when the temperature decreased by around 6°C, and silencing upon rewarming to 34°C (Figs. 1, 5). These low-background activity, high-threshold (LB-HT) cold thermoreceptor terminals represented 28% of the total number of cold-sensitive terminals. Table 2 summarizes the firing characteristics for these LB-HT cold terminals. Peak frequency and temperature at which cold-evoked firing appeared were significantly lower than in HB-LT

TABLE 2. Values of the Different Parameters of the NTI Response Measured in HB-LT and LB-HT Cold Terminals

NTI Activity Parameter	Cold Terminal Type	
	HB-LT	LB-HT
Success, %	6	3
Background activity*, imp·s ⁻¹	6.6 ± 1.0 <i>n</i> = 26	0.5 ± 0.1 <i>n</i> = 9
Cooling threshold*, °C	32.1 ± 0.2 <i>n</i> = 26	28.2 ± 0.5 <i>n</i> = 9
Cooling response*, imp·s ⁻¹	34.4 ± 2.3 <i>n</i> = 26	6.3 ± 1.2 <i>n</i> = 9
Silencing temperature, °C	23.1 ± 0.9 <i>n</i> = 26	17.1 ± 1.1 <i>n</i> = 9
Mechanical stimulation, No. NTI/10 s		
Before	39.0 ± 15.9 <i>n</i> = 6	6.3 ± 1.8 <i>n</i> = 3
During	74.1 ± 17.0 <i>n</i> = 6	25.3 ± 6.0 <i>n</i> = 3
Heating response, No. NTI/30 s		
Before	56.8 ± 16.3 <i>n</i> = 6	7.8 ± 2.7 <i>n</i> = 4
During	355.5 ± 111.4 <i>n</i> = 6	32.3 ± 11.0 <i>n</i> = 4
Menthol response, Δ imp·s ⁻¹	9.5 ± 6.9 <i>n</i> = 2	5.5 ± 3.1 <i>n</i> = 3

Success % indicates the percentage of successful attempts of recording a terminal from each group with regard to the total number of attempts. Background activity, cooling threshold, cooling response, and silencing temperature (see Methods) are measured during a cooling ramp. Mechanical and heating response are expressed as the total number of NTIs immediately before and during the mechanical pulse and heating ramp (in 10 and 30 seconds, respectively). Menthol response is expressed as the increment of activity during menthol perfusion with regard to the 30 seconds immediately before starting menthol perfusion. The statistical analyses were made comparing the values of HB-LT with LB-HT using a Student's *t*-test.

* *P* < 0.01.

cold thermoreceptor terminals (cf. Figs. 5, 6). In five LB-HT terminals where a 30-second heating ramp was applied, a discharge of impulses (mean 32.3 ± 11.1 NTIs, *n* = 4) was evoked (Fig. 5) with a mean duration of 13.9 ± 5.6 seconds. Also, three out of the five LB-HT terminals tested fired NTIs in response to mechanical stimulation (Table 2).

Three out of four LB-HT tested for sensitivity to a 3-minute application of menthol (20 μM) at 34°C had a marked increase of ongoing activity from 0.7 ± 0.2 to 6.1 ± 3.1 imp·s⁻¹ (*n* = 3). Moreover, in all four units treated with menthol, this agent decreased cold threshold to a cooling ramp from 28.1 ± 0.2°C to 30.4 ± 0.8°C, *n* = 4. In two LB-HT terminals explored for sensitivity to a 397 mOsm·kg⁻¹ hyperosmolar solution at 34°C, NTI frequency approximately doubled compared to the pretreatment activity (data not shown).

DISCUSSION

In this study, we confirmed that the mouse cornea is innervated by trigeminal ganglion (TG) neurons, which respond to the same stimulus modalities as those of other mammalian species, and characterized them as mechanonociceptor, polymodal nociceptor, and cold thermoreceptor sensory nerve terminals. We also defined electrophysiologically two distinct classes of cold thermoreceptor endings whose activity may underlie, respectively, basal and irritation-evoked tearing and blinking.

Functional categorization of corneal receptor terminals was performed, selecting the population of terminals that exhibited spontaneous activity or responded positively to mechanical pressure before the electrode was moved to the next recording point. Mechanosensitive terminals were subsequently tested for responsiveness to thermal and chemical stimuli in order to define their polymodality. Hence, this recording strategy does not recruit “silent nociceptors,” that is, sensory neurons that are not excited by physiological stimuli, even at potentially tissue-damaging intensities, but develop nerve impulse activity when inflammation develops,³⁷ and whose existence in the eye has been suggested.³⁸

Corneal polymodal nociceptor neurons are the most frequently encountered functional type of sensory nerve terminal in the cat and guinea pig cornea, where they represent around 65% of the total number of corneal nerve fibers.^{21–25} Comparatively, polymodal nociceptors appear to be less abundant (approximately 40%) in the mouse. Mechanonociceptors comprise 15% and 12% of all corneal sensory fibers in the cat and guinea pig, respectively,^{23–25} and only 9.5% in mice, while the percentage of cold thermoreceptors identified in the mouse is almost double that found in the cat (17%) and the guinea pig (21%).^{23–25}

Such variability in the proportion of modality-specific sensory fibers can be attributed to species differences; however, it may also reflect the bias introduced by the use of different identification methods to sample the sensory modality of corneal sensory nerve fibers. The percentage of axons of a given modality has been generally calculated based on their presence in extracellular recordings of single nerve fibers dissected from the ciliary nerves at the back of the eye, in anesthetized cats or in excised and superfused guinea pig eyes.^{22,33} In both cases, thinly myelinated A-delta mechanosensory fibers tend to be picked up more easily than the unmyelinated (C) fibers that are in most cases polymodal nociceptor and cold fibers.^{24,33,36} In contrast, the technique used to record from single corneal nerve terminals *in vitro* in guinea pig or mouse eyes favors the detection of thin cold thermoreceptor terminals, which display spontaneous activity, are more superficially located, and branch more extensively than polymodal and mechanoreceptor endings, thus producing larger-amplitude NTIs.^{17,24,26–28,33,34,39,40} In the present work, we tried to confront this caveat through a systematic sampling of impulse activity at regularly distributed points on the corneal surface, thus reaching theoretically all types of nerve terminals. Only terminals that were unambiguously identified were counted. Hence, the data obtained in mice corneas probably provide a reasonably accurate picture of the relative proportion of terminals of different modality in this species. Still, the group of unidentified terminals, containing units of very low amplitude or not responding clearly to any of the stimuli, may include an unknown proportion of “silent nociceptors.”

The method used for application of mechanical force to the corneal surface precluded an accurate measurement of force threshold of purely mechanoreceptor endings, which has been reported to be higher than in polymodal nociceptor endings.^{21,24} Still, the short-lasting discharge of NTIs evoked by a sustained pressure in these terminals suggests that they belong to the general class of high-threshold, phasic mechanonociceptive primary sensory neurons also identified in the cornea of the cat and guinea pig.^{23–25,33,34} The transducing channels conferring mechanosensitivity to these endings have not been identified yet, although expression of the mechanosensory channel Piezo2⁴¹ has been reported in approximately 30% of corneal TG neurons. This Piezo2-positive subpopulation of neurons possesses an immunocytochemical profile very different from canonical cold or

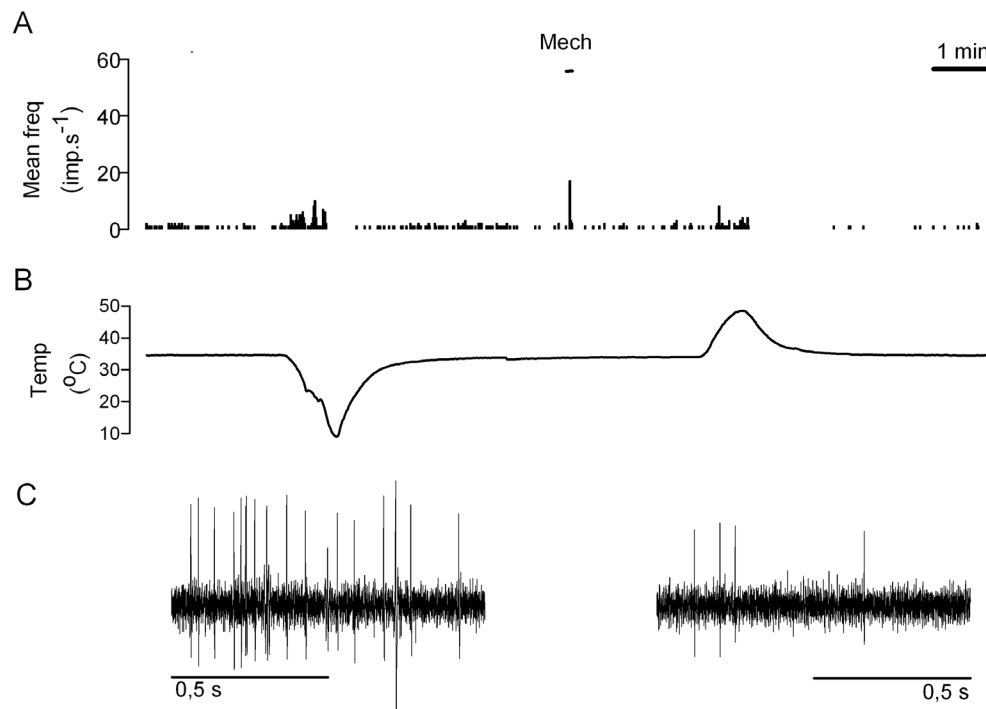


FIGURE 5. Example of the NTI response of a LB-HT cold thermoreceptor terminal. **(A)** Time histogram of the NTI discharge. Mech, mechanical stimulation (10- μ m forward displacement of the electrode for 2 seconds). **(B)** Bath temperature trace during the time period shown in **(A)**. **(C)** Sample records of the NTI impulse activity during the cooling ramp (*left*) and the heating ramp (*right*) in the same LB-HT terminal.

polymodal nociceptor neurons, thus suggesting that they may correspond functionally to pure mechanonociceptive neurons.⁴² It could be further speculated that the morphologically distinct group of corneal nerve terminals named

“ramified endings”³⁹ are given by this group of corneal mechanonociceptor neurons. The recent finding of a selective expression of Nav1.1 channels in high-threshold mechanosensitive fibers of the skin opens new venues for a more

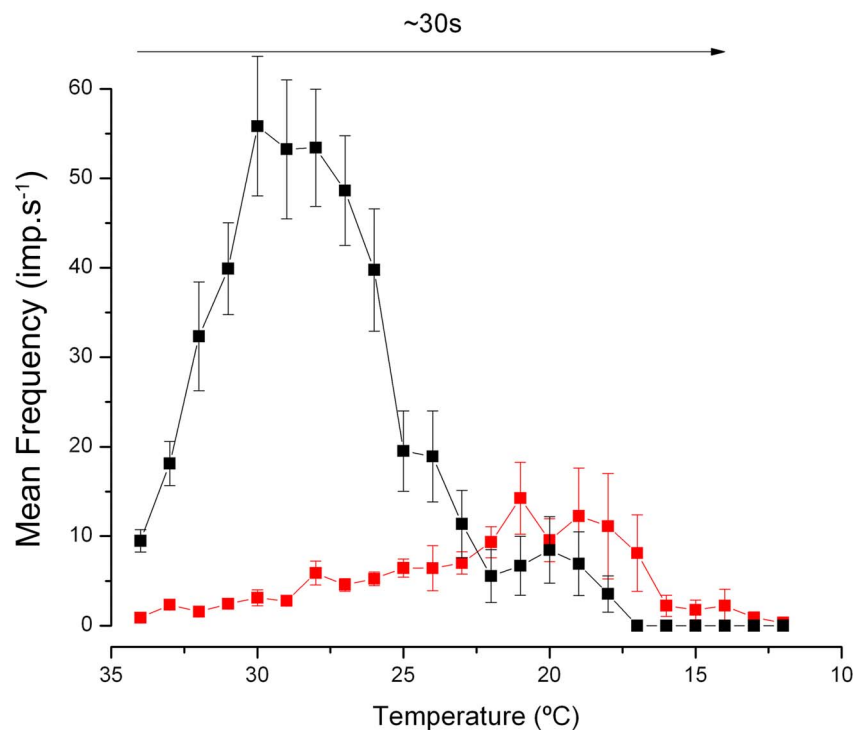


FIGURE 6. Stimulus-response curves of HB-LT and LB-HT cold-sensitive terminals. Mean NTI firing frequency values (imp.s⁻¹) are represented versus temperature during a cooling ramp from 34°C to 12°C in ~30 seconds, as indicated by the *horizontal arrow*. *Black squares*, HB-LT terminals ($n = 26$). *Red squares*, LB-HT terminals ($n = 9$).

precise identification of the transducing mechanisms in corneal pure mechanosensory terminals.⁴³

Corneal polymodal nociceptors of the mouse responded unambiguously with a NTI discharge to mechanical stimuli, noxious heating, and capsaicin and were sensitized by a mixture of inflammatory agents. Their frequency rises with osmolality increases to discrete values; however, it is well established that firing frequency values over 0.5 imp·s⁻¹ in polymodal human nerve fibers already evoke conscious pain sensations.^{44,45} Thus, it seems reasonable to assume that activation of corneal polymodal terminals produced by the different stimuli used in our study would also evoke pain sensation in the awake mouse.

The sensitivity to heating and capsaicin supports the presence of TRPV1 channels, the molecular integrator of noxious heat, and a large variety of algesic substances⁴⁶⁻⁴⁸ in this class of nerve terminals. The presence of TRPV1 channels in corneal polymodal nociceptors contributing to ocular surface pain is to be expected from the strong tearing and blinking response evoked by application of capsaicin to the eye in many species including mice.^{17,49} A smaller proportion of polymodal terminals was also activated by the TRPA1 channel agonist AITC, which also evokes irritative tearing and blinking when applied to mouse eyes.¹⁷ Nonetheless, the low number of polymodal terminals responding to TRPA1 activation in mice, as also seen in guinea pigs,³³ suggests that TRPA1 channels are not highly expressed in corneal polymodal nociceptor endings.

Altogether, mouse polymodal nociceptors innervating the cornea are functionally very similar to polymodal fibers of the mouse skin or tongue^{18,50,51} and of the cornea of other species.^{22,23,25} They encode approximately the intensity of mechanical stimuli, develop inactivation/sensitization upon repeated noxious stimulation, and respond to a large variety of endogenous and exogenous chemicals.^{38,52}

Our study confirms with functional data the dense innervation of the mouse cornea by cold thermoreceptor axon terminals, evidenced by recent immunocytochemical studies.^{17,39,48} Canonical low-threshold cold thermoreceptors of various species and tissues are easily recognized by their regular background impulse activity at the normal temperature of the tissue, whose frequency of discharge changes with temperature oscillations of 1°C or less.^{23,24,28,53,54} We distinguished in the mouse cornea a high number of HB-LT cold terminals that typically responded to static and dynamic changes in temperature and were activated by menthol and hyperosmotic stimuli, as reported for canonical cold thermoreceptors of the cornea and of various other tissues in many species.^{19,32,54-57} In the eye, it has been postulated that these low-threshold corneal thermoreceptors detect small temperature changes linked to interblink tear film evaporation, thereby providing a tonic sensory input to the brain encoding wetness of the eye surface.^{17,29,58,59}

The additional presence in the cornea of a subpopulation of unmyelinated cold thermoreceptor axons responding only to strong cooling and osmolality was originally reported in the cat in 1993 by Gallar et al.,²⁴ who named them “cold” nociceptors. More recently, corneal “dry-sensitive” neurons responding to weak or strong levels of ocular surface desiccation, hyperosmolarity, and menthol and exhibiting parallel high or low sensitivity to corneal cooling were reported in the TG of the rat.^{30,32,60} Here, we unambiguously identified and characterized these two subclasses of cold-thermosensitive neurons in the mouse cornea and propose their inclusion within the general class of cold thermoreceptor primary sensory neurons.

The sensitivity of cold thermoreceptor neurons to low temperatures is primarily determined by the expression of

TRPM8, a nonselective cationic channel gated by moderate cold and also by menthol and hyperosmolar solutions.^{19,61,62} TRPM8 channel opening contributes to an excitatory, depolarizing current in sensory neurons named I_{cold} that triggers propagated impulse responses to cooling (for review see Refs. 63, 64). It has been shown that the cell bodies of cold-thermosensitive neurons in dorsal root and trigeminal sensory ganglia display a wide range of thresholds for cold stimuli.⁶⁵⁻⁶⁹ This heterogeneity of cooling thresholds is determined to large extent by variability in the density of TRPM8 channels, but is also attributed to the absence or limited expression of the potassium channels Kv1.1-1.2.^{70,71} These K⁺ channels sustain an outward current termed I_{KD} in most primary sensory neurons that opposes the inward current generated by cold activation of TRPM8, thereby acting as an excitability break that prevents unspecific cold-induced depolarization.⁶⁵ In TG cold-sensitive neurons in culture, it has been convincingly demonstrated that low-threshold cold thermoreceptor neurons virtually lack I_{KD}, while in high-threshold cold thermoreceptor neurons, which respond only to stronger cooling, this current is prominent.⁷¹ Accordingly, cold threshold and cooling-evoked firing rate in cold thermoreceptor sensory neurons depend on a balance between the expression levels of TRPM8 and Kv1 channels.^{65,71,72} Therefore, it is conceivable that HB-LT cold thermoreceptor terminals of the mouse cornea belong to TG cold-sensitive neurons presenting a high expression of TRPM8 channels and low or no expression of Kv1 channels, whereas LB-HT terminals originate from TG cold-sensitive neurons with lower levels of TRPM8 channels and a significant presence of Kv1 channels.^{70,71}

It is worth noting that the two subtypes of corneal cold thermoreceptor terminals found in the mouse cornea also responded to stimuli such as heat, osmolality changes, mechanical forces, menthol, and a variety of other irritant agents. A variable sensitivity of canonical cold thermoreceptors to these stimuli has been reported earlier.^{17-19,24,29,30,32,35,55} This is not exceptional. Other classes of peripheral somatosensory receptors equipped with specific transducing channels that confer preferential sensitivity for a particular form of stimulating energy, also express transduction channels for other stimulus qualities.⁷³ Our data suggest that this is a prominent characteristic of corneal cold thermoreceptors, where the expression of multiple transduction channels equips the ocular surface with a set of sensory receptors particularly tuned for the detection of the main physical parameters associated with changes in corneal surface wetness (temperature, osmolality, cell shrinking).⁵⁹

It is generally accepted that corneal mechanonociceptor axons, preferentially tuned to fire phasically in response to mechanical stimulation, and polymodal nociceptors tonically activated by a large variety of noxious chemical, mechanical, and thermal stimuli, are the peripheral substrate of acute and chronic eye pain.^{52,74} Second-order neurons of this pathway are mainly located at the caudal levels of the spinal trigeminal nucleus, in the transition area between nucleus caudalis and cervical spinal cord (Vc/C1).⁷⁵⁻⁷⁷ In contrast, there is considerable evidence that a majority of corneal HB-LT cold thermoreceptors project to second-order neurons located at the transition zone between the spinal trigeminal subnucleus caudalis and subnucleus interpolaris (Vi/Vc), an area proposed as the processing center for neural regulation of lacrimation and blinking via the superior salivatory nucleus (SSN) and the facial motor nucleus.^{20,32,78} The SSN and facial motor nucleus also receive an input from Vc/C1 neurons connected to corneal nociceptors for reflex motor and autonomic ocular responses evoked by injurious stimuli.^{77,79} The location in the brainstem of the second-order neurons connecting with LB-HT cold thermoreceptors is not certain. Kurose and Meng²⁰

reported the activation of a subset of second-order neurons of the Vi/Vc region only by strong cooling. These neurons were also activated by acidic stimulation of the cornea, suggesting that they may receive inputs from both LB-HT and polymodal nociceptor corneal fibers. In conditions such as experimental chronic eye dryness where the LB-HT cold thermoreceptors become selectively sensitized,^{20,31,36,80} there is enhanced neural activity in ocular responsive neurons in both the Vi/Vc and Vc/C1 regions.⁸⁰ It has been suggested that LB-HT neurons contribute importantly to discomfort sensations accompanying chronic eye surface dryness.^{36,59} Hence it is tempting to speculate that this subclass of cold thermoreceptor primarily projects into nociceptor-driven second-order neurons of the Vc/C1 region evoking discomfort and, also together with the polymodal nociceptors reaching that area, on the neurons of the Vi/Vc involved in the regulation of tearing and blinking.

Under normal environmental conditions, it has been postulated that small changes in ocular surface temperature and osmolality resulting from tear fluid evaporation at the exposed eye surface are encoded by HB-LT cold thermoreceptors^{17,23,24,28,29,35,58,59} and transmitted to second-order Vi/Vc neurons.^{20,78} When there is excessive evaporation and/or hyperosmolarity of tear film, the LB-HT cold thermoreceptors may also be recruited, and evoke a sense of irritation through the same pain-labeled pathways as corneal mechano- and polymodal nociceptor nerve fibers. These three sensory receptors types may also be activated by cell shrinkage and local inflammation caused by dryness. Together, this multi-receptor sensory message evokes augmented tearing and blinking as well as the irritative, unpleasant dryness sensations associated with chronic dry eye.^{36,59} A similar, variable involvement of the different functional classes of peripheral sensory receptors is expected to occur after injury or pathologic processes affecting the ocular surface.

Electrophysiological classification of somatosensory receptor types, based both on the form of energy to which they preferentially respond and on the stimulus intensity required for their activation, has been a useful approach to correlate stimulus modalities and activation of specific sets of peripheral sensory neurons leading to qualitatively distinct sensations, but has a number of technical limitations. Repeated application of different stimuli may cause tissue damage, favoring the apparition of inactivation, fatigue, or sensitization.⁸¹ This is particularly true for polymodal nociceptors, whose stimulus threshold is by definition close to injurious intensities. The discovery in sensory receptor neurons of specific membrane transducing molecules for different forms of energy⁸²⁻⁸⁴ served as an essential tool to refine the identification of peripheral receptor classes. Still, there is considerable variability in transducing molecule expression within neurons of the same functional receptor category; moreover, neurons with peripheral terminals responding preferentially to a specific stimulus often express also transducing molecules for other stimulus modality.^{70,85} Although the functional specificity of the various populations of primary sensory neuron for a particular class of stimulus is well defined, this molecular promiscuity determines their potential excitation by other modalities of stimuli, particularly under abnormal conditions. It is conceivable that the molecular heterogeneity of neurons belonging to a general functional type may be, at least in part, behind the striking variability of the peripheral sensory messages generated at ocular surface tissues under pathological conditions, including inflammation and injury.

The present work has been performed in mice, an experimental model particularly suitable to study the molecular basis of eye surface sensations. It defines in this species the electrophysiological characteristics of the different classes of

sensory nerve endings innervating the cornea, providing new data that can in our view be used for a multidisciplinary approach to the study of normal and pathological eye sensations.

Acknowledgments

The authors thank Rodolfo Madrid for the contribution to the preparation of corneal nerve terminal recording in the mouse. For critical reading of the manuscript, they also thank James A. Brock. In addition they thank Enol Artime and Paola Braga for their technical assistance.

Supported by Grants FC-15-GRUPIN14-141 from the Consejería de Economía y Empleo del Gobierno del Principado de Asturias, Spain, cosponsored with FEDER funds from the European Union and the Fundación Ramón Areces, Caja Rural de Asturias, and Ministerio de Economía y Competitividad of Spain and FEDER (SAF2014-54518-C3-1-R and SAF2014-54518-C3-2-R). C.B. acknowledges financial support from the Spanish State Research Agency, through the "Severo Ochoa" Programme for Centres of Excellence in R&D (SEV-2013-0317).

Disclosure: **O. González-González**, None; **F. Bech**, None; **J. Gallar**, None; **J. Merayo-Llives**, None; **C. Belmonte**, None

References

- Namavari A, Chaudhary S, Sarkar J, et al. In vivo serial imaging of regenerating corneal nerves after surgical transection in transgenic thy1-YFP mice. *Invest Ophthalmol Vis Sci.* 2011; 52:8025-8032.
- Wang C, Fu T, Xia C, Li Z. Changes in mouse corneal epithelial innervation with age. *Invest Ophthalmol Vis Sci.* 2012;53: 5077-5084.
- Reichard M, Weiss H, Poletti E, et al. Age-related changes in murine corneal nerves. *Curr Eye Res.* 2015;1-8.
- Marfurt CF, Murphy CJ, Florczak JL. Morphology and neurochemistry of canine corneal innervation. *Invest Ophthalmol Vis Sci.* 2001;42:2242-2251.
- Muller LJ, Marfurt CF, Kruse F, Tervo TMT. Corneal nerves: structure, contents and function. *Exp Eye Res.* 2003;76:521-542.
- de Castro F, Silos-Santiago I, Lopez de Armentia M, Barbacid M, Belmonte C. Corneal innervation and sensitivity to noxious stimuli in trkA knockout mice. *Eur J Neurosci.* 1998;10:146-152.
- Guaquil VH, Pan Z, Karagianni N, Fukuoka S, Alegre G, Rosenblatt MI. VEGF-B selectively regenerates injured peripheral neurons and restores sensory and trophic functions. *Proc Natl Acad Sci U S A.* 2014;111:17272-17277.
- Shevalye H, Yorek MS, Coppey LJ, et al. Effect of enriching the diet with menhaden oil or daily treatment with resolvin D1 on neuropathy in a mouse model of type 2 diabetes. *J Neurophysiol.* 2015;114:199-208.
- Íñigo-Portugués A, Alcalde I, Gonzalez-Gonzalez O, Gallar J, Belmonte C, Merayo-Llives J. Decreased basal tear in aged mice is linked to morphological and functional changes in corneal sensory nerve fibers. *Acta Ophthalmol.* 2014;92.
- Cai D, Zhu M, Petroll WM, Koppaka V, Robertson DM. The impact of type 1 diabetes mellitus on corneal epithelial nerve morphology and the corneal epithelium. *Am J Pathol.* 2014; 184:2662-2670.
- Pal-Ghosh S, Pajoohesh-Ganji A, Tadvalkar G, et al. Topical Mitomycin-C enhances subbasal nerve regeneration and reduces erosion frequency in the debridement wounded mouse cornea. *Exp Eye Res.* 2015;146:361-39.
- Pajoohesh-Ganji A, Pal-Ghosh S, Tadvalkar G, Kyne BM, Saban DR, Stepp MA. Partial denervation of sub-basal axons persists

- following debridement wounds to the mouse cornea. *Lab Invest.* 2015;95:1305-1318.
13. Hu K, Harris DL, Yamaguchi T, Von Andrian UH, Hamrah P. A dual role for corneal dendritic cells in herpes simplex keratitis: local suppression of corneal damage and promotion of systemic viral dissemination. *PLoS One.* 2015;10:1-23.
 14. Chucair-Elliott AJ, Zheng M, Carr DJJ. Degeneration and regeneration of corneal nerves in response to HSV-1 infection. *Invest Ophthalmol Vis Sci.* 2015;56:1097-1107.
 15. Esquenazi S, He J, Li N, Bazan NG, Esquenazi I, Bazan HEP. Comparative in vivo high-resolution confocal microscopy of corneal epithelium, sub-basal nerves and stromal cells in mice with and without dry eye after photorefractive keratectomy. *Clin Experiment Ophthalmol.* 2007;35:545-549.
 16. Bian F, Pelegri FSA, Pflugfelder SC, Volpe EA, Li D-Q, de Paiva CS. Desiccating stress-induced MMP production and activity worsens wound healing in alkali-burned corneas. *Invest Ophthalmol Vis Sci.* 2015;56:4908-4918.
 17. Parra A, Madrid R, Echevarria D, et al. Ocular surface wetness is regulated by TRPM8-dependent cold thermoreceptors of the cornea. *Nat Med.* 2010;16:1396-1399.
 18. Zhang X, Mak S, Li L, et al. Direct inhibition of the cold-activated TRPM8 ion channel by G α q. *Nat Cell Biol.* 2012;14:851-858.
 19. Quallo T, Vastani N, Horridge E, et al. TRPM8 is a neuronal osmosensor that regulates eye blinking in mice. *Nat Commun.* 2015;6:7150.
 20. Kurose M, Meng ID. Corneal dry-responsive neurons in the spinal trigeminal nucleus respond to innocuous cooling in the rat. *J Neurophysiol.* 2013;109:2517-2522.
 21. Belmonte C, Giraldez F. Responses of cat corneal sensory receptors to mechanical and thermal stimulation. *J Physiol.* 1981;321:355-368.
 22. Giraldez F, Geijo E, Belmonte C. Response characteristics of corneal sensory fibers to mechanical and thermal stimulation. *Brain Res.* 1979;177:571-576.
 23. Belmonte C, Gallar J, Pozo MA, Rebollo I. Excitation by irritant chemical substances of sensory afferent units in the cat's cornea. *J Physiol.* 1991;437:709-725.
 24. Gallar J, Pozo MA, Tuckett RP, Belmonte C. Response of sensory units with unmyelinated fibres to mechanical, thermal and chemical stimulation of the cat's cornea. *J Physiol.* 1993;468:609-622.
 25. Brock JA, McLachlan EM, Belmonte C. Tetrodotoxin-resistant impulses in single nociceptor nerve terminals in guinea-pig cornea. *J Physiol.* 1998;512:211-217.
 26. Brock JA, Pianova S, Belmonte C. Differences between nerve terminal impulses of polymodal nociceptors and cold sensory receptors of the guinea-pig cornea. *J Physiol.* 2001;533:493-501.
 27. Carr RW. The effects of polarizing current on nerve terminal impulses recorded from polymodal and cold receptors in the guinea-pig cornea. *J Gen Physiol.* 2002;120:395-405.
 28. Carr RW. Effects of heating and cooling on nerve terminal impulses recorded from cold-sensitive receptors in the guinea-pig cornea. *J Gen Physiol.* 2003;121:427-439.
 29. Hirata H, Meng ID. Cold-sensitive corneal afferents respond to a variety of ocular stimuli central to tear production: implications for dry eye disease. *Invest Ophthalmol Vis Sci.* 2010;51:3969-3976.
 30. Hirata H, Oshinsky ML. Ocular dryness excites two classes of corneal afferent neurons implicated in basal tearing in rats: involvement of transient receptor potential channels. *J Neurophysiol.* 2012;107:1199-1209.
 31. Hirata H, Rosenblatt MI. Hyperosmolar tears enhance cooling sensitivity of the corneal nerves in rats: possible neural basis for cold-induced dry eye pain. *Invest Ophthalmol and Vis Sci.* 2014;55:5821-5833.
 32. Kurose M, Meng ID. Dry eye modifies the thermal and menthol responses in rat corneal primary afferent cool cells. *J Neurophysiol.* 2013;110:495-504.
 33. Acosta MC, Luna C, Quirce S, Belmonte C, Gallar J. Changes in sensory activity of ocular surface sensory nerves during allergic keratoconjunctivitis. *Pain.* 2013;154:2353-2362.
 34. Acosta MC, Luna C, Quirce S, Belmonte C, Gallar J. Corneal sensory nerve activity in an experimental model of UV keratitis. *Invest Ophthalmol Vis Sci.* 2014;55:3403-3412.
 35. Parra A, Gonzalez-Gonzalez O, Gallar J, Belmonte C. Tear fluid hyperosmolality increases nerve impulse activity of cold thermoreceptor endings of the cornea. *Pain.* 2014;155:1481-1491.
 36. Kovacs I, Luna C, Quirce S, et al. Abnormal activity of corneal cold thermoreceptors underlies the unpleasant sensations in dry eye disease. *Pain.* 2016;157:399-417.
 37. Michaelis M, Habler HJ, Jaenig W. Silent afferents: a separate class of primary afferents? *Clin Exp Pharmacol Physiol.* 1996;23:99-105.
 38. Belmonte C, Viana F. Transduction and encoding of noxious stimuli. In: Schmidt RF, Willis W, eds. *Encyclopedia of Pain.* Vol. 2513. Berlin: Springer-Verlag; 2007:2515-2528.
 39. Ivanusic JJ, Wood RJ, Brock JA. Sensory and sympathetic innervation of the mouse and guinea pig corneal epithelium. *J Comp Neurol.* 2013;521:877-893.
 40. Carr RW, Pianova S, McKemy DD, Brock JA. Action potential initiation in the peripheral terminals of cold-sensitive neurones innervating the guinea-pig cornea. *J Physiol.* 2009;587:1249-1264.
 41. Ranade SS, Woo SH, Dubin AE, et al. Piezo2 is the major transducer of mechanical forces for touch sensation in mice. *Nature.* 2014;516:121-125.
 42. Bron R, Wood RJ, Brock JA, Ivanusic JJ. Piezo2 expression in corneal afferent neurons. *J Comp Neurol.* 2014;522:2967-2979.
 43. Osteen JD, Herzig V, Gilchrist J, et al. Selective spider toxins reveal a role for the Nav1.1 channel in mechanical pain. *Nature.* 2016;534:494-499.
 44. Gybels J, Handwerker HO, Van Hees J. A comparison between the discharges of human nociceptive nerve fibres and the subject's ratings of his sensations. *J Physiol.* 1979;292:193-206.
 45. Yarnitsky D, Simone DA, Dotson RM, Cline MA, Ochoa JL. Single C nociceptor responses and psychophysical parameters of evoked pain: effect of rate of rise of heat stimuli in humans. *J Physiol.* 1992;450:581-592.
 46. Caterina MJ, Schumacher MA, Tominaga M, Rosen TA, Levine JD, Julius D. The capsaicin receptor: a heat-activated ion channel in the pain pathway. *Nature.* 1997;389:816-824.
 47. Julius D. TRP channels and pain. *Annu Rev Cell Dev Biol.* 2013;29:355-384.
 48. Alamri A, Bron R, Brock JA, Ivanusic JJ. Transient receptor potential cation channel subfamily V member 1 expressing corneal sensory neurons can be subdivided into at least three subpopulations. *Front Neuroanat.* 2015;9:71.
 49. Gonzalez GG, De la Rubia PG, Gallar J, Belmonte C. Reduction of capsaicin-induced ocular pain and neurogenic inflammation by calcium antagonists. *Invest Ophthalmol Vis Sci.* 1993;34:3329-3335.
 50. Reeh PW. Sensory receptors in mammalian skin in an in vitro preparation. *Neurosci Lett.* 1986;66:141-146.
 51. Meseguer V, Alpizar YA, Luis E, et al. TRPA1 channels mediate acute neurogenic inflammation and pain produced by bacterial endotoxins. *Nat Commun.* 2014;5:3125.

52. Belmonte C, Tervo T, Gallar J. Sensory innervation of the eye. In: Levin LA, Nilsson SFE, Ver Hoeve J, Wu S, Kaufman PL, Aim A, eds. *Adler's Physiology of the Eye*. Amsterdam: Elsevier; 2011:363-384.
53. Hensel H. Neural processes in thermoregulation. *Physiol Rev*. 1973;53:948-1017.
54. Braun HA, Bade H, Hensel H. Static and dynamic discharge patterns of bursting cold fibers related to hypothetical receptor mechanisms. *Pflugers Arch*. 1980;386:1-9.
55. Hensel H, Zotterman Y. The effect of menthol on the thermoreceptors. *Acta Physiol Scand*. 1951;24:27-34.
56. Orio P, Parra A, Madrid R, González O, Belmonte C, Viana F. Role of Ih in the firing pattern of mammalian cold thermoreceptor endings. *J Neurophysiol*. 2012;108:3009-3023.
57. Olivares E, Salgado S, Maidana JP, et al. TRPM8-dependent dynamic response in a mathematical model of cold thermoreceptor. *PLoS One*. 2015;10:e0139314.
58. Belmonte C, Gallar J. Cold thermoreceptors, unexpected players in tear production and ocular dryness sensations. *Invest Ophthalmol Vis Sci*. 2011;52:3888-3892.
59. Belmonte C, Acosta MC, Merayo-Llodes J, Gallar J. What causes eye pain? *Curr Ophthalmol Rep*. 2015;3:111-121.
60. Hirata H, Fried N, Oshinsky ML. Quantitative characterization reveals three types of dry-sensitive corneal afferents: pattern of discharge, receptive field, and thermal and chemical sensitivity. *J Neurophysiol*. 2012;108:2481-2493.
61. McKemy DD, Neuhauss WM, Julius D. Identification of a cold receptor reveals a general role for TRP channels in thermosensation. *Nature*. 2002;416:52-58.
62. Dhaka A, Murray AN, Mathur J, Earley TJ, Petrus MJ, Patapoutian A. TRPM8 is required for cold sensation in mice. *Neuron*. 2007;54:371-378.
63. Latorre R, Brauchi S, Madrid R, Orio P. A cool channel in cold transduction. *Physiology*. 2011;26:273-285.
64. Almaraz L, Manenschijn J-A, de la Pena E, Viana F. TRPM8. *Handb Exp Pharmacol*. 2014;222:547-579.
65. Viana F, de la Pena E, Belmonte C. Specificity of cold thermotransduction is determined by differential ionic channel expression. *Nat Neurosci*. 2002;5:254-260.
66. Nealen ML, Gold MS, Thut PD, Caterina MJ. TRPM8 mRNA is expressed in a subset of cold-responsive trigeminal neurons from rat. *J Neurophysiol*. 2003;90:515-520.
67. Thut PD, Wrigley D, Gold MS. Cold transduction in rat trigeminal ganglia neurons in vitro. *Neuroscience*. 2003;119:1071-1083.
68. Babes A, Zorzon D, Reid G. Two populations of cold-sensitive neurons in rat dorsal root ganglia and their modulation by nerve growth factor. *Eur J Neurosci*. 2004;20:2276-2282.
69. Teichert RW, Raghuraman S, Memon T, et al. Characterization of two neuronal subclasses through constellation pharmacology. *Proc Natl Acad Sci U S A*. 2012;109:12758-12763.
70. Madrid R, Donovan-Rodríguez T, Meseguer V, Acosta MC, Belmonte C, Viana F. Contribution of TRPM8 channels to cold transduction in primary sensory neurons and peripheral nerve terminals. *J Neurosci*. 2006;26:12512-12525.
71. Madrid R, de la Peña E, Donovan-Rodríguez T, Belmonte C, Viana F. Variable threshold of trigeminal cold-thermosensitive neurons is determined by a balance between TRPM8 and Kv1 potassium channels. *J Neurosci*. 2009;29:3120-3131.
72. Viana F. Chemosensory properties of the trigeminal system. *ACS Chem Neurosci*. 2011;2:38-50.
73. Belmonte C, Viana F. Molecular and cellular limits to somatosensory specificity. *Mol Pain*. 2008;4:14.
74. Belmonte C, Aracil A, Acosta MC, Luna C, Gallar J. Nerves and sensations from the eye surface. *Ocul Surf*. 2004;2:248-253.
75. Meng ID, Hu JW, Benetti AP, Bereiter DA. Encoding of corneal input in two distinct regions of the spinal trigeminal nucleus in the rat: cutaneous receptive field properties, responses to thermal and chemical stimulation, modulation by diffuse noxious inhibitory controls, and projections to the parabrachial area. *J Neurophysiol*. 1997;77:43-56.
76. Hirata H, Hu JW, Bereiter DA. Responses of medullary dorsal horn neurons to corneal stimulation by CO(2) pulses in the rat. *J Neurophysiol*. 1999;82:2092-2107.
77. Bereiter DA, Okamoto K, Tashiro A, Hirata H. Endotoxin-induced uveitis causes long-term changes in trigeminal subnucleus caudalis neurons. *J Neurophysiol*. 2005;94:3815-3825.
78. Hirata H, Okamoto K, Tashiro A, Bereiter DA. A novel class of neurons at the trigeminal subnucleus interpolaris/caudalis transition region monitors ocular surface fluid status and modulates tear production. *J Neurosci*. 2004;24:4224-4232.
79. Katagiri A, Thompson R, Rahman M, Okamoto K, Bereiter DA. Evidence for TRPA1 involvement in central neural mechanisms in a rat model of dry eye. *Neuroscience*. 2015;290:204-213.
80. Rahman M, Okamoto K, Thompson R, Katagiri A, Bereiter DA. Sensitization of trigeminal brainstem pathways in a model for tear deficient dry eye. *Pain*. 2015;156:942-950.
81. Mountcastle VB. Physiology of sensory receptors: introduction to sensory processes. In: Mountcastle VB. *Medical Physiology*. 12th ed, Vol. II. St. Louis: Mosby; 1968:1341-1375.
82. Gees M, Owsianik G, Nilius B, Voets T. TRP channels. *Compr Physiol*. 2012;2:563-608.
83. Zhang X. Molecular sensors and modulators of thermoreception. *Channels (Austin)*. 2015;9:73-81.
84. Hao J, Bonnet C, Amsalem M, Ruel J, Delmas P. Transduction and encoding sensory information by skin mechanoreceptors. *Pflugers Arch*. 2015;467:109-119.
85. Belmonte C, Brock JA, Viana F. Converting cold into pain. *Exp Brain Res*. 2009;196:13-30.